

Magnetic properties of iron-rich Fe-Zr glasses

D. H. Ryan and J. M. D. Coey

Department of Pure and Applied Physics, Trinity College, Dublin 2, Ireland

E. Batalla, Z. Altounian, and J. O. Ström-Olsen

Rutherford Physics Building, McGill University, 3600 University Street, Montreal, Quebec, Canada H3A 2T8

(Received 29 July 1986; revised manuscript received 22 December 1986)

A systematic study of the magnetic properties of melt-spun amorphous $\text{Fe}_x\text{Zr}_{100-x}$ alloys with $88 \leq x \leq 93$ using Mössbauer and magnetization measurements has established the magnetic phase diagram. The ordering temperature T_c falls sharply with increasing x ; below a second transition T_{xy} , associated with the freezing of transverse-spin components, all the alloys order asperomagnetically ($T_{xy} < T_c$). Hysteresis appears at still lower temperatures, but it is not directly related to the transverse-spin freezing. A $T^{1.3}$ variation of hyperfine field observed for $T < T_{xy}$ is attributed to excitation of transverse magnetic modes. Contrary to the predictions of Heisenberg spin-glass theory, neither the ferromagnetic nor the asperomagnetic order appears to be long range. Extrapolation to $x=100$ indicates that pure amorphous iron would be a speromagnet with an iron moment of $1.7\mu_B$ and a spin-freezing temperature of order 150 K. Upon hydrogenation the magnetic structures of all the α -Fe-Zr alloys lose their noncollinear character, becoming good ferromagnets with Curie points in excess of 400 K.

I. INTRODUCTION

Iron-rich amorphous binary alloys exhibit some novel magnetic properties. These alloys may be considered as amorphous iron stabilized by the inclusion of small, controlled amounts of impurities. The general formula is $\text{Fe}_x\text{M}_{100-x}$, where $x \geq 85$ and M may be an early transition metal (Y, Zr, Hf, . . .) or a metalloid (B, . . .). A question of interest is whether extrapolation to $x=100$ for different systems yields the same magnetic properties, which could then be identified as those of pure amorphous iron, or if different systems extrapolate to distinct magnetic states which might then be associated with different polymorphs of amorphous iron,¹ analogous to the bcc, fcc, and hcp polymorphs of crystalline iron which exhibit quite different magnetic behavior.²

The atomic moment and magnetic ordering temperature (T_c) of binary amorphous iron alloys increase steadily from zero at a critical concentration which is usually near $x \simeq 40$. In ferromagnetic systems, the Curie temperature rises to a maximum and then begins to drop sharply as $x \rightarrow 100$. The maximum is at 750 K and $x=70$ for $M=\text{B}$,³ at 270 K and $x=85$ for $M=\text{Zr}$,⁴ and at 300 K and $x=87$ for $M=\text{Hf}$.⁵ The system with $M=\text{Y}$ behaves differently; α - $\text{Fe}_x\text{Y}_{100-x}$ alloys are not collinear ferromagnets at any concentration;⁶ they are asperomagnets with a random, noncollinear spin structure in which there is a tendency for parallel alignment of neighboring spins.⁷ The spin-freezing temperature rises slowly with increasing x , and appears to saturate at about 110 K as $x \rightarrow 100$.

Hiroyoshi and Fukamichi were the first to suggest that α - $\text{Fe}_{100-x}\text{Zr}_x$ alloys with $x \simeq 90$ were not simple ferromagnets.⁸ They proposed a transition to a spin-glass phase on the basis of the appearance of irreversible susceptibility well below T_c . Their susceptibility data have

been reproduced by several other workers.⁹⁻¹² Some of these authors, Read *et al.*^{10,13} and Beck and Kronmüller,¹² reject a spin-glass transition, attributing the irreversibility to the normal increase in coercivity and associated magnetic hardness expected in ferromagnets at low temperatures. Kaul⁹ found that the $x=90$ alloy behaves like a weak itinerant ferromagnet in that it exhibits a quadratic (T^2) decrease of magnetization with temperature. However, Beck and Kronmüller¹² showed that the T^2 dependence gives way to a $T^{3/2}$ law if measurements are made in fields ≥ 0.37 T.

It has been noted that the magnetization of an $x=90$ alloy fails to saturate at 4.2 K in fields of 15 T,¹⁴ as a result, values deduced from measurements in lower fields are unusually low for a concentrated iron alloy [(1-1.5) $\mu_B/\text{Fe atom}$], and they fall sharply as $x \rightarrow 100$.^{1,15} Our earlier extrapolation of Mössbauer data at $T \geq 80$ K to $T=0$ suggested collapse not only of the magnetization, but also of the hyperfine field as $x \rightarrow 100$.¹ This conclusion was mistaken for reasons that will become apparent in Secs. III A and IV B. We had also reported a reversible transition from a ferromagnetic to an asperomagnetic state when an $x=89$ alloy was cooled below 60 K.¹⁶ Mössbauer spectra at 4.2 K in an applied field indicate a random spin arrangement at this temperature.^{17,18} Support for the idea that there is some sort of random spin freezing is provided by the neutron measurements of Rhyne and Fish.¹⁹ On a sample with $x=91$, they find that the spin-correlation length below T_c saturates at 2.2 nm, with no sign of long-range ferromagnetic order. One study of the critical exponents yielded values that are quite different from those at a normal ferromagnetic phase transition,²⁰ but in another investigation the usual values for a three-dimensional (3D) Heisenberg system were reported.²¹

As most of the previous studies were carried out on alloys of a single composition, we felt that a systematic study of materials prepared over the entire range accessible by melt spinning was needed to resolve the confusion surrounding the magnetic properties of this system. Although it is only possible to prepare iron-rich $a\text{-Fe}_x\text{Zr}_{100-x}$ over a narrow composition range by this method ($88 \leq x \leq 93$), it is just in this range that the most significant variation in magnetic properties takes place. We have spun several series of $\text{Fe}_x\text{Zr}_{100-x}$ alloys with $88 \leq x \leq 93$ in steps of 1 at. %. These have been studied by Mössbauer spectroscopy and magnetization measurements in fields up to 19 T, to determine both the total moment and its z component. Furthermore, ac susceptibility has been used to determine the magnetic transition temperatures, and magnetic structures have been deduced from Mössbauer spectroscopy in an external field.

Hydrogen has a profound influence on both the ordering temperature and the magnetic structure of iron-rich amorphous alloys.^{16,22-26} In $a\text{-Fe}_x\text{Y}_{100-x}$ it converts asperomagnetic alloys into soft ferromagnets with a greatly increased ordering temperature,^{22,26} while in $a\text{-Fe}_x\text{Zr}_{100-x}$ it increases T_c and eliminates the "spin-glass" transition.^{16,24} These effects may be related to dilation of the noncrystalline lattice by hydrogen, or to changes in electronic structure which entrain increased ferromagnetic exchange and enhanced iron moments. Hydrogenated $a\text{-Fe}_x\text{Zr}_{100-x}$ alloys have been included in our study principally to serve as ferromagnetic reference materials against which the magnetic properties of the unhydrogenated alloys may be judged.

II. EXPERIMENTAL DETAILS

Alloys of the required composition were prepared by argon-arc melting of 99.9%-pure elements, followed by melt spinning under helium. Meter-length ribbons, 1–2 mm wide and 10–20 μm thick, were obtained. Sample quality was verified by differential scanning calorimetry and x-ray diffraction.²⁷ No traces of any crystalline phases were found on either surface; specifically, the (110)

and (200) $\alpha\text{-Fe}$ reflections²⁵ were absent. Crystallization takes place between 800 and 900 K (Ref. 27) (Table I).

A vibrating-sample magnetometer operated between 4.2 and 80 K in fields of up to 5 T provided most of the magnetization curves. Some data in fields of up to 19 T were obtained at the Service Nationale des Champs Intenses, Grenoble. Magnetic ordering temperatures were determined by measuring the ac susceptibility χ_{ac} as a function of temperature. Mössbauer spectra were obtained between 4.2 and 290 K using a conventional constant-acceleration spectrometer and a $^{57}\text{CoRh}$ source. Measurements in an applied field were made using an 8-T superconducting magnet. The same samples were used for both the Mössbauer and magnetization measurements, so that direct comparisons could be made without any possibility of error from variations in quality or composition along the ribbons.

Samples were electrolytically charged with hydrogen using an arsenic-doped potassium carbonate solution.²⁴ Hydrogen content and desorption characteristics were determined by thermopiezic analysis.²⁸

III. RESULTS

A. $\text{Fe}_x\text{Zr}_{100-x}$

Earlier work has established that the magnetic ordering temperature T_c rises from zero at a critical concentration of $x = 38$ and peaks at about 270 K in the region $x = 85$.⁴ For the range of samples we studied it fell sharply from 265 K at $x = 88$ to 163 K at $x = 93$; values obtained by ac susceptibility were in agreement with those determined by the kink-point method in small dc fields and by thermal scans of Mössbauer absorption at zero velocity. The linear extrapolation of T_c shown in Fig. 1 would suggest an ordering temperature close to 0 K for pure amorphous iron, but we believe this extrapolation is misleading, for the reasons explained in Sec. IV B.

All of the samples exhibit a measurable high-field slope in their 4.2-K magnetization curves, which is particularly evident in samples with $x \geq 90$ (Fig. 2). The component

TABLE I. Summary of the magnetic properties of $a\text{-Fe}_x\text{Zr}_{100-x}$ with and without hydrogen. χ_∞ , the high field susceptibility was measured in a field of 5 T, except for the value marked by * measured in 19 T. The crystallization temperature, T_x , was obtained at a heating rate of 40 K/min (Ref. 27).

x (at. %)	T_c (K)	M_z ($\mu_B/\text{Fe atom}$)		B_{hf} (T)		χ_∞ ($\text{J/T}^2 \text{kg}^{-1}$)	B_c (mT)	T_x (K)
		4.2 K	80 K	4.2 K	80 K			
88 (as made)	265.5	1.60 \pm 0.01	22.3 \pm 0.2	25.9 \pm 0.2		0.9 \pm 0.2	0.7 \pm 0.1	882 \pm 5
88 (hydrogenated)		2.19				<0.5		882 \pm 5
89 (as made)	244	1.59	22.2	25.7		1.1	0.9	884
89 (hydrogenated)	400 \pm 20	1.97		29.1		<0.5		884
90 (as made)	226	1.56	21.4	25.5		1.3	2.9	867
90 (hydrogenated)	380	2.06				<0.2		867
91 (as made)	215	1.54	20.4	25.9		1.9	5.5	874
91 (hydrogenated)		2.00		29.7				874
92 (as made)	186	1.23	17.0	25.6		5.3	17.1	848
92 (hydrogenated)		1.99				<0.02*		848
93 (as made)	163	0.58	16.0	25.7		2.6	74	806
93 (hydrogenated)		1.99		28.8		<0.1	0.4	806

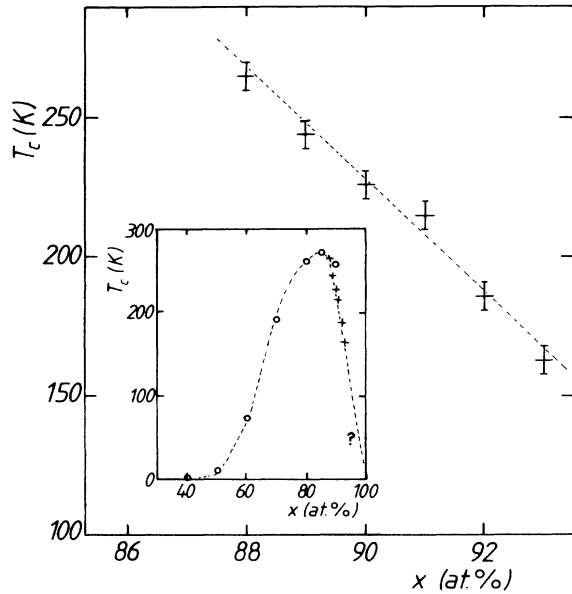


FIG. 1. Ordering temperature vs x for iron-rich $a\text{-Fe}_x\text{Zr}_{100-x}$. Inset: behavior of T_c over full composition range; this work (+) and Ref. 4 (o).

M_z of the magnetization which saturates readily is defined by extrapolating the data for $1 \leq B_0 \leq 4$ T to $B_0 = 0$. Slopes, together with the z components of the iron moments, are listed in Table I. It should be noted that the ferromagnetic component of the moment decreases rapidly for $x \geq 90$. A high-field slope is evident up to the highest fields (19 T) for $a\text{-Fe}_{90}\text{Zr}_{10}$ and $a\text{-Fe}_{92}\text{Zr}_8$.

All unhydrogenated samples exhibit some hysteresis at 4.2 K, and the loops narrow with increasing temperature. Data for the $x = 93$ sample are shown in Fig. 3. The coercive field increases rapidly below 50 K, and its value at a given temperature increases with x . These points are illustrated in the insets of Fig. 3. The isothermal remanance at 4.2 K was observed to decrease slowly with time

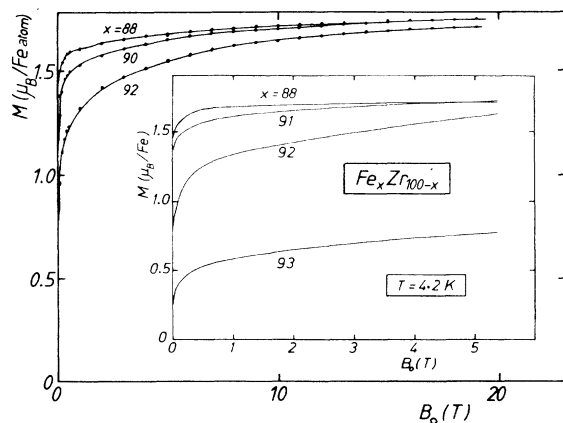


FIG. 2. Magnetization curves at 4.2 K for $a\text{-Fe}_x\text{Zr}_{100-x}$, in 19 T, and inset, 5 T.

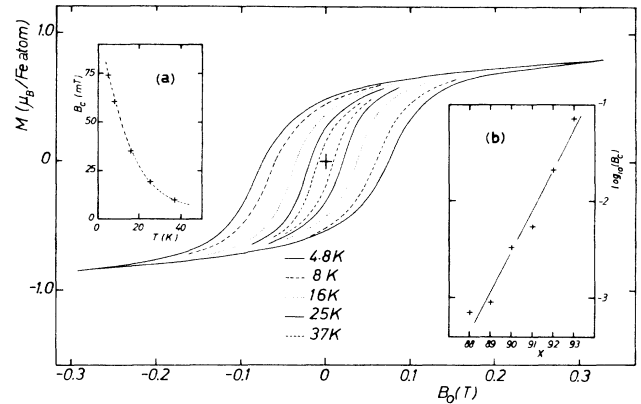


FIG. 3. Hysteresis loops for $a\text{-Fe}_{93}\text{Zr}_7$ at various temperatures. Insets: (a) Coercivity vs T for $a\text{-Fe}_{93}\text{Zr}_7$; (b) coercivity vs x at 4.2 K for $a\text{-Fe}_x\text{Zr}_{100-x}$.

and could be fitted to a $\ln(t)$ law over a range of 1–10 000 s.

Mössbauer spectra were obtained for all samples as a function of temperature between 4.2 and ~ 290 K [room temperature (RT)]. Data taken at 4.2 K are shown in Fig. 4. These are magnetically split, with extremely broad lines typical of amorphous systems with wide distributions of hyperfine fields (B_{hf}). The spectra were fitted using two methods: (i) by assuming a Lorentzian distribution of B_{hf} , and (ii) by using the window Fourier expansion method²⁹ or the histogram method to obtain B_{hf} distributions. The average hyperfine fields, $\langle B_{\text{hf}} \rangle$, measured at 80 and 4.2 K, are shown in Fig. 5, along with the moments derived from magnetization data. Normally, the hyperfine field is roughly proportional to the iron moment and the conversion factor $15 \text{ T}/\mu_B$, valid for bcc iron, was assumed in drawing the right-hand scales in Figs. 5 and 10. The decline in $\langle B_{\text{hf}} \rangle$ with increasing iron content seen at 80 K, together with magnetization data, earlier suggested to us a collapse of the iron moment.¹ However *no decline is apparent at 4.2 K*, where the field is essentially constant at 25.5 ± 0.3 T across the whole composition range examined, giving an atomic moment on the iron of roughly $1.7\mu_B$. Since the magnetization (Fig. 2) is always significantly less, it follows that none of these alloys have a collinear magnetic structure in the ground state. Another important point is that $\langle B_{\text{hf}} \rangle$ falls more rapidly with increasing temperature than would be expected for a normal ferromagnet [Fig. 6(a)]. In the range $4.2 \text{ K} \leq T \leq T_c/2$ the variation is

$$[\langle B_{\text{hf}}(0) \rangle - \langle B_{\text{hf}}(T) \rangle] / B_{\text{hf}}(0) \propto (T/T_c)^\eta, \quad (1)$$

with $\eta = 1.3 \pm 0.1$ for $x = 89$ and 93 [Fig. 6(b)].

Much of the analysis in the Discussion is based on the values of magnetization and *average* hyperfine field. Hyperfine-field distributions determined from the 4.2-K Mössbauer spectra by method (ii) are included in Figs. 4 and 9. A variable 3:1 intensity of the three line pairs was used; we find $r = 2$ for the unhydrogenated alloys. Besides the main peak in the $P(B_{\text{hf}})$ distribution, corresponding to an iron moment of $1.7\mu_B$, there appears to be

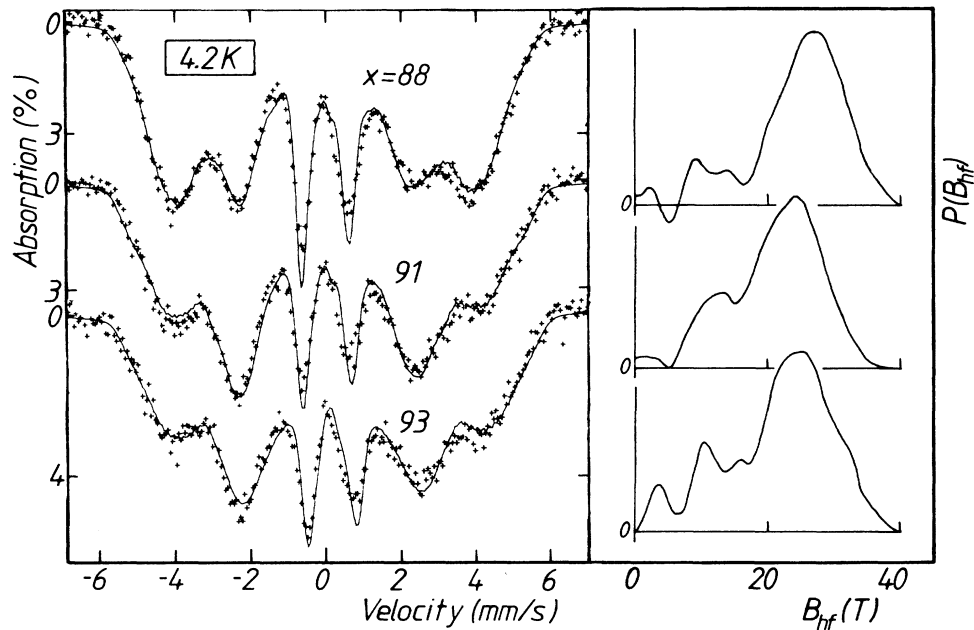


FIG. 4. Mössbauer spectra at 4.2 K for $\text{Fe}_x\text{Zr}_{100-x}$.

some evidence of a subsidiary maximum corresponding to a moment of $0.7\mu_B$.³⁰

B. $\text{Fe}_x\text{Zr}_{100-x}\text{H}_y$

Samples of iron-rich α -Fe-Zr are easily charged with hydrogen by electrolysis to values of y of order 20. The

hydrogen is released over a period of a few days at 20°C or directly at around 120°C when heated at 20°C/min (Fig. 7). Magnetic ordering temperatures are estimated to be in the region of 400 K, but the desorption of hydrogen makes accurate determination impossible.

Figure 8 shows that at 4.2 K the hydrogenated materials are good soft ferromagnets, readily saturating in 0.1 T, with no measurable high-field slope. The extrapolated moments have increased to around $2\mu_B/\text{Fe}$ atom, in agreement with Mössbauer data.

The Mössbauer spectra at 4.2 K are independent of x . One is shown in Fig. 9. They are similar to those of the untreated samples, except that the values of $\langle B_{\text{hf}} \rangle$ are appreciably greater. These are plotted, along with moments derived from the magnetization curves, in Fig. 10.

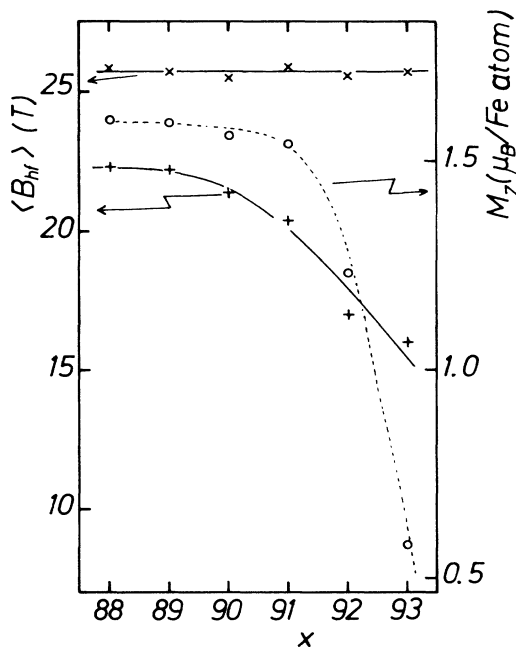


FIG. 5. $\langle B_{\text{hf}} \rangle$ at 80 K (+) and 4.2 K (x), together with moments M_z deduced from magnetization measurements at 4.2 K (o).

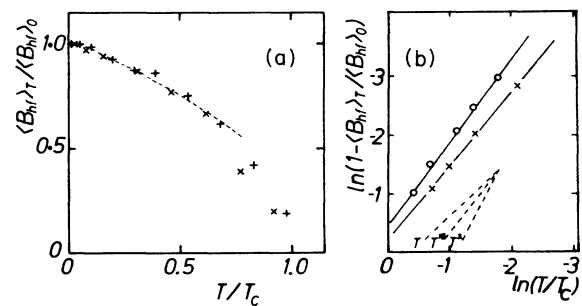


FIG. 6. (a) Reduced $\langle B_{\text{hf}} \rangle$ vs reduced temperature for α - $\text{Fe}_{93}\text{Zr}_7$ (x), $\text{Fe}_{91}\text{Zr}_9$ (+), and $\text{Fe}_{89}\text{Zr}_{11}$ (o). The dotted line shows the $(T/T_c)^{1.3}$ variation. (b) Plot to deduce the power η in Eq. (1). Slopes for $\eta = 1, \frac{1}{2},$ and 2 are indicated.

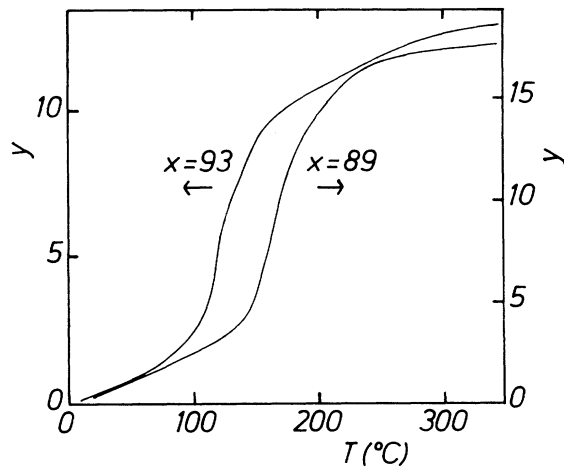


FIG. 7. Typical thermal-desorption curves for hydrogenated $\text{Fe}_x\text{Zr}_{100-x}\text{H}_y$. Sample masses were ≈ 1.5 mg.

IV. DISCUSSION

A. Magnetic ground state

What is the nature of the magnetic order? Materials which exhibit a large high-field slope in their $T \approx 0$ K magnetization curves and do not attain the saturation magnetization expected for the atomic moments deduced from their hyperfine field cannot be collinear ferromagnets. Noncollinearity is confirmed directly by the persistence of lines 2 and 5 observed previously in the Mössbauer spectrum of an $x = 91$ sample in a field of 2.5 T,¹⁷ and shown in Fig. 13 for an $x = 92$ sample in a field of 2 T. The discrepancy (Fig. 5) between the total iron moment, deduced from the 4.2-K Mössbauer data to be

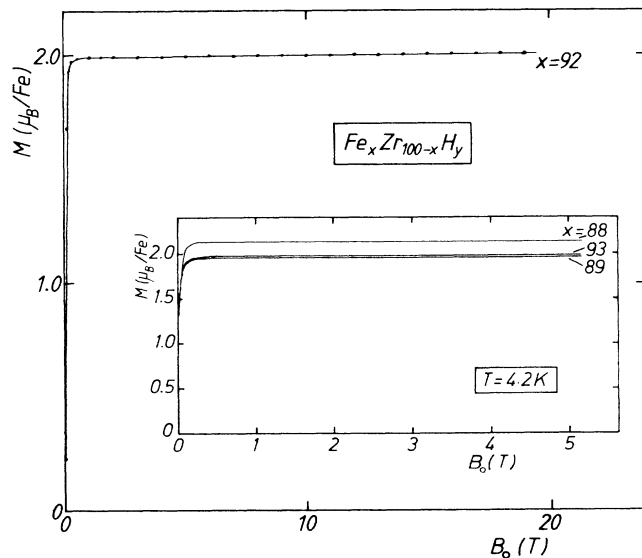


FIG. 8. Magnetization curves at 4.2 K for $a\text{-Fe}_x\text{Zr}_{100-x}\text{H}_y$, in 19 T and inset, 5 T.

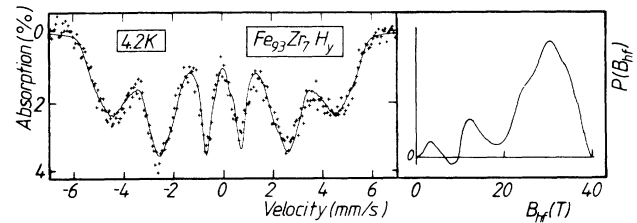


FIG. 9. Mössbauer spectrum at 4.2 K for $a\text{-Fe}_{93}\text{Zr}_7\text{H}_y$.

$1.7\mu_B$ for the whole series, and its z component, deduced by extrapolating magnetization curves to zero applied field, becomes larger as x increases, but it exists also for $x \leq 91$ (Fig. 5). To envisage the extent of the noncollinearity, let us consider a model where the iron moments are oriented randomly within a cone of half-angle ψ about some locally preferred direction; ψ is 35° for $x = 88$ and increases to 110° for $x = 93$. The cone picture need not be taken literally, but there exists some sort of asperomagnetic structure⁷ with a random anisotropic distribution of moment directions, and hence a nonzero magnetization within a domain. In other words, the z components of the moments lie near a common direction within the domain, while the x and y components are frozen at random in the perpendicular plane. Such a picture will make sense, provided λ_c , the domain size (or equivalently, the correlation length of the ferromagnetic component), is significantly greater than the interatomic distance. The domain must include enough atoms to permit the definition of a principal axis along which the net moment is a maximum; this net moment should be much greater than the $\sqrt{N}\mu$ expected if the random distribution of moment directions were isotropic (N is the number of atoms in the domain and μ is the atomic moment).

Amorphous $\text{Fe}_x\text{Zr}_{100-x}$ alloys with $88 \leq x \leq 93$ are among the best examples of asperomagnets we have yet encountered. There is a large low-field susceptibility which is practically indistinguishable from that of a

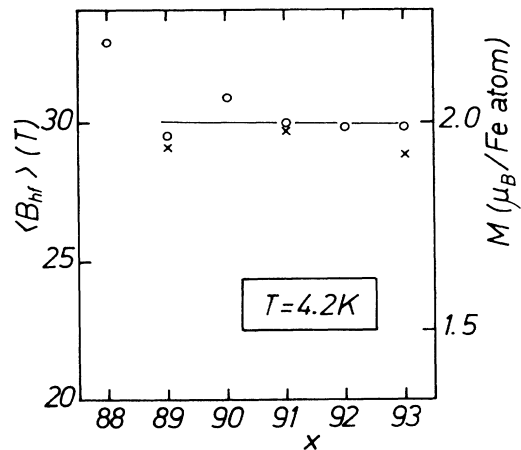


FIG. 10. $\langle B_{\text{hf}} \rangle$ (\times) and moments deduced from magnetization measurements at 4.2 K (\circ), for $a\text{-Fe}_x\text{Zr}_{100-x}\text{H}_y$.

demagnetization-limited ferromagnet in our experiments (except when hysteresis effects become important). The first part of the magnetization corresponding to alignment of the magnetic axes of all the domains along the external field indicates that N is large (≥ 1000). The observation by Rhyne and Fish¹⁹ of a 2.2-nm correlation length, almost independent of temperature, in an $x = 91$ alloy, implies that $N \approx 600$.

The reason for the noncollinear magnetic structures in α -Fe-Zr must be antiferromagnetic exchange; this is the only plausible explanation of the large fields needed to align the iron moments completely. Single-ion anisotropy, which is important in rare-earth amorphous alloys,⁷ cannot be significant here in view of the hydrogen-induced ferromagnetism (Fig. 8).

B. Amorphous iron

We find no evidence for anything other than a smooth change in magnetic structure with composition. None of the alloys studied is a collinear ferromagnet. We suppose that an increasing proportion of negative exchange interactions with increasing x leads to the precipitous fall in T_c (Fig. 1) and the increasingly noncollinear magnetic structures. Negative exchange is likely to be associated with shorter Fe—Fe bonds.^{20,31} Extrapolation to $x = 100$ is fairly straightforward for the hyperfine field and the corresponding iron atomic moment. The 4.2-K data in Fig. 5 lead us to expect that pure amorphous iron would have a moment of about $1.7\mu_B$. Prediction of its magnetic structure and ordering temperature, however, is more delicate. It is unreasonable to extrapolate the magnetic ordering temperature to ≈ 0 K at $x = 100$ if the iron retains its moment. Increasingly antiferromagnetic exchange in an amorphous magnet will eventually lead to speromagnetic order (isotropic random spin freezing).⁷ Furthermore, reentrant spin-glass theory³² suggests that the spin-freezing temperature remains constant beyond the point where the irreversibility line and the Curie-temperature line meet (see Sec. IV D). From the phase diagram in Fig. 11 it is seen that these lines meet at about 150 K. We therefore suggest that pure amorphous iron will be speromagnetic with a spin-freezing temperature of about 150 K. A similar conclusion has been arrived at independently in a recent study of the ac susceptibility of the α -Fe_xZr_{100-x} system.³³

C. Excitations

In Fig. 6 we see that the hyperfine field at low temperatures drops faster than $T^{3/2}$ with increasing temperature. This was noted previously in the α -Fe_xY_{100-x} system,⁶ and examination of published data on AuFe (Ref. 34) and certain mixed oxides (Ref. 35) seems to show the same behavior. All these systems are asperomagnets or ferromagnetic spin glasses at low temperature. It is tempting to associate the temperature dependence of the iron moment with a normal $T^{3/2}$ term due to excitation of ferromagnetic spin waves plus a T term due to low-temperature excitations of the transverse-spin components. Mizutani *et al.*³⁶ have reported a large linear term in the low-temperature specific heat of amorphous Fe_xZr_{100-x}

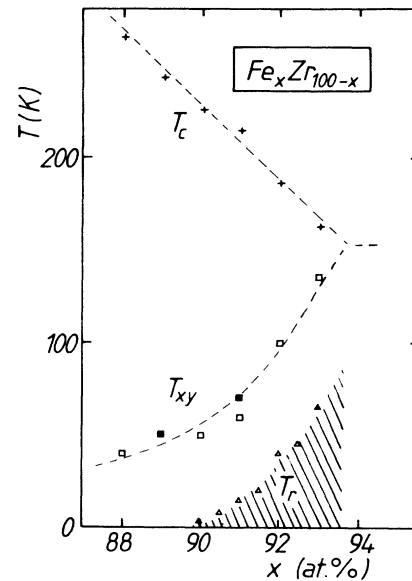


FIG. 11. Magnetic phase diagram for α -Fe_xZr_{100-x}, showing a T_c (+) and T_{xy} (\square), and upon the appearance of coercivity at T_r (\triangle). Solid symbols are from the present work, \square from Ref. 40 and \triangle from Ref. 10.

($88 \leq x \leq 92$). This γT term, with $\gamma \approx 25$ mJ/mol K⁻², is far too large to be of electronic origin, but its magnitude is quite consistent with the magnetic specific heat expected from the temperature decrease in magnitude of the iron moment. Our own specific-heat measurements, however, show nonergodic behavior below T_r ;³⁷ the specific heat appears to increase with time on the 100-ms timescale of the measurement. The effect disappears when the samples are hydrogenated (i.e., purely ferromagnetic). Since the Mössbauer spectra are acquired over periods of order 10^5 s, the variations in Fig. 6 are expected to represent the equilibrium situation.

D. Is there a spin-glass transition?

Many authors have observed that there exists a temperature below T_c which is marked by the onset of irreversible susceptibility.⁸⁻¹² This temperature, which decreases with increasing field, we will call T_{xy} for reasons to be explained. Some of our own data on the $x = 93$ sample are shown in Fig. 12. As explained in the Introduction, there is controversy concerning the interpretation of such data; certain authors^{8,9,11} see evidence for a transition from a ferromagnetic state for $T_c > T > T_{xy}$ to a spin-glass state below T_{xy} , whereas for others^{10,12,13} the irreversibility is a consequence of the normal growth of hysteresis and coercivity expected for a ferromagnet at low temperatures. Note that the thermoremanent magnetization in Fig. 12 is almost precisely equal to the difference between the field-cooled and zero-field-cooled magnetizations.

The hysteresis explanation is attractive, and may well apply to others of the "reentrant-spin-glass" systems that have been reported since the original theoretical work of Sherrington and Kirkpatrick.^{38,39} However, we must re-

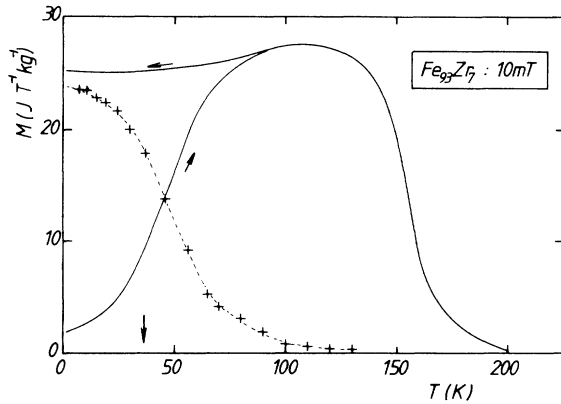


FIG. 12. Thermomagnetic curves for $a\text{-Fe}_{93}\text{Zr}_7$. Dotted line shows remanence of a field-cooled sample, heated in zero field. Arrow indicates temperature at which the coercivity equals the measuring field.

ject it for $a\text{-Fe}_x\text{Zr}_{100-x}$ upon examination of the data in Figs. 3 and 12, which were obtained with exactly the same experimental setup. The field used in Fig. 12 was 10 mT, and the onset of irreversibility is at 85 K, but, as seen from Fig. 3, the coercivity only reaches 10 mT at 33 K; it falls exponentially with temperature and should be negligible at 85 K, where the magnetization begins to depend on the sample history.

A clue to the interpretation of T_{xy} is provided by comparing the temperature variation of the frozen iron moment with that of its z component obtained from magnetization data in fields of less than 1 T, which largely suffice to eliminate domains, but do not modify the asperomagnetic structure. For alloys with $x = 89, 91,$ and 93 , the $M(T)$ and $\langle B_{\text{hf}} \rangle(T)$ curves meet at approximately the same temperature as the onset of irreversibility, T_{xy} . It seems that only the z component of the moment is nonzero for $T_c > T > T_{xy}$, whereas the transverse components only begin to block below T_{xy} . To confirm this we have examined Mössbauer spectra of the $x = 92$ sample in either region in a field of 2 T applied parallel to the γ direction. This is sufficient to overcome the demagnetizing effect of the sample and align the z components of the iron moments. Results are shown in Fig. 13. At 120 and 80 K, above T_{xy} , the frozen components of the spins are aligned with the field, but below T_{xy} , the $\Delta m_I = 0$ transitions (lines 2 and 5) become apparent as the transverse-spin components freeze.

To summarize, we draw the magnetic phase diagram of $a\text{-Fe}_x\text{Zr}_{100-x}$, Fig. 11, which shows the main transitions, T_c and T_{xy} , from various measurements. We also show a third line, for the temperature T_r , where the coercivity exceeds an arbitrary value of 3 mT.

There are striking similarities between the magnetic phase diagram for iron-rich $a\text{-Fe}_x\text{Zr}_{100-x}$ ($88 \leq x \leq 93$) and the crystalline $\text{Fe}_x\text{Au}_{100-x}$ system in the concentrated spin-glass regime $15 \leq x \leq 20$,⁴⁰ once one allows for the opposite signs of dT_c/dx .

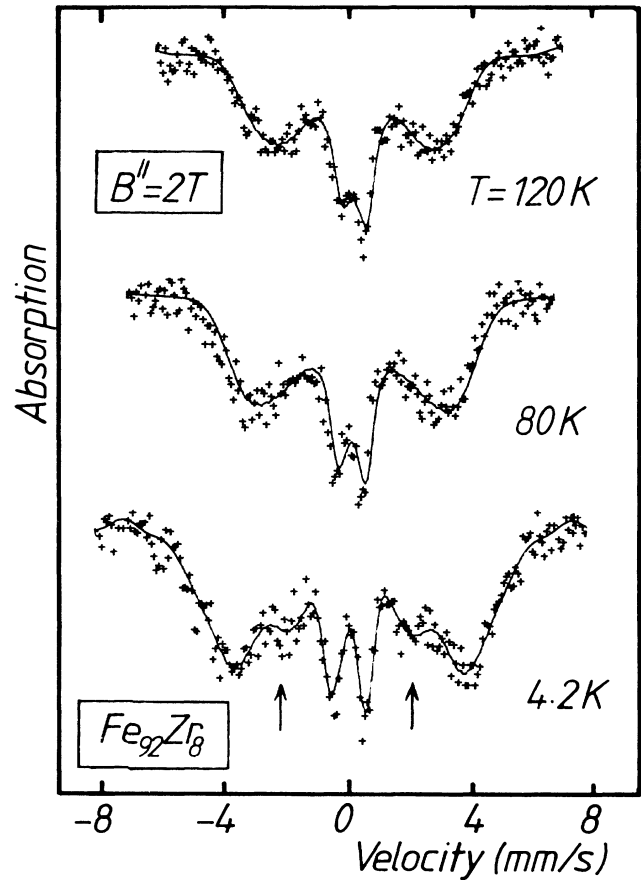


FIG. 13. Mössbauer spectra of $a\text{-Fe}_{92}\text{Zr}_8$ in an applied field of 2 T, at 120, 80, and 4.2 K.

E. Comparison with theory

There are also similarities between Fig. 11 and theoretical predictions of Heisenberg spin glasses. When the exchange distribution is sufficiently biased toward positive (ferromagnetic) values, these theories³² predict a sequence of transitions upon descending temperature from a paramagnetic to ferromagnetic to ferromagnetic spin glass with weak irreversibility to ferromagnetic spin glass with strong irreversibility (replica symmetry breaking—the A - T line). These transitions might be associated with T_c , T_{xy} , and the appearance of coercivity, respectively. T_{xy} should be defined in the limit of very small applied field, but the appearance of coercivity is not a well-defined transition because coercivity declines exponentially with temperature. The choice of 3 mT in Fig. 11 is arbitrary.

Rather than entering a claim that our experiments confirm Heisenberg spin-glass theory, we prefer to point out where our data and those of others who have worked on $a\text{-Fe}_x\text{Zr}_{100-x}$ seems to be at variance with the theory. (i) There is considerable doubt as to whether T_c represents a proper ferromagnetic phase transition. It seems to shade continuously away from one with increasing x . Magnetic broadening appears in the Mössbauer spectra

more than 50 K above the ordering temperature determined by ac susceptibility and critical exponents. Critical exponents measured by Yamauchi *et al.*²⁰ deviate from the values expected for the 3D Heisenberg model. Taken together with the 2.2-nm correlation length of Rhyne and Fish for $x = 91$,¹⁹ these data indicate that the ferromagnetic phase of iron-rich $a\text{-Fe}_x\text{Zr}_{100-x}$ below T_c is only ferromagnetic in a limited sense, the moments being aligned over domains of dimension 2–3 nm, as shown in Fig. 14(a). It is a “wandering-axis ferromagnet” and sensitive permeability measurements on toroidal samples should be able to confirm this. From our type of magnetization data, a long-period helimagnet such as MnSi (Ref. 41) would be practically indistinguishable from a normal ferromagnet. However, on this point it should be noted that Kaul *et al.*²¹ have recently reported normal 3D Heisenberg-model exponents for $a\text{-Fe}_x\text{Zr}_{100-x}$ with $x = 91$. The critical behavior may therefore depend on sample preparation. (ii) There is a more or less well-defined temperature T_{xy} where the transverse-spin components freeze (judged by comparison of the temperature dependence of the total moment with that of its z component). T_{xy} appears to coincide with the onset of irreversibility in small dc fields.⁴² The magnetic order becomes asperomagnetic below T_{xy} , but in zero field the domain size remains that of the ferromagnetic phase. (iii) Hysteresis appears at temperatures which are clearly lower than T_{xy} , but one cannot define a unique temperature T for its appearance because it varies exponentially with T [Fig. 3, inset (a), and Ref. 13].

V. CONCLUSIONS

Extrapolations from iron-rich $a\text{-Fe}_x\text{Zr}_{100-x}$ to $x = 100$ indicate that pure amorphous iron would have an iron moment of $\sim 17\mu_B$ and that it would order speromagnetically below a freezing temperature of ~ 150 K. The magnetic phase diagram shows two transition lines. Below T_c the alloys exhibit short-range ferromagnetic order, with a correlation length or domain size that decreases with increasing x . The transition at T_{xy} corresponds to random freezing of the transverse-spin components to give short-range asperomagnetic order with the same domain size. Hysteresis and coercivity appear at lower temperatures, and are not directly related to the transverse-

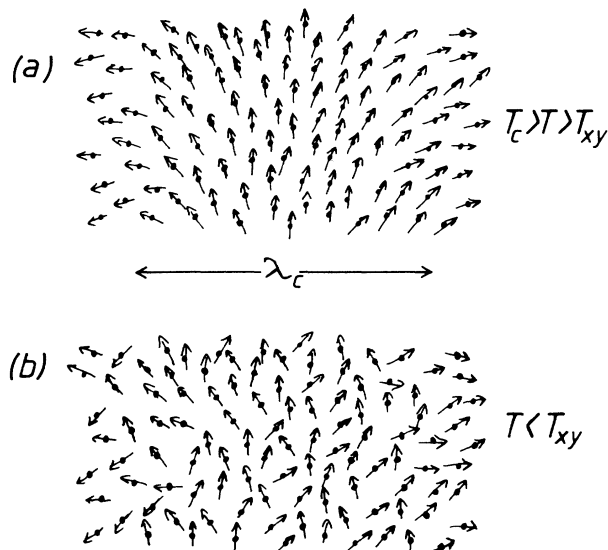


FIG. 14. Spin structures (a) above and (b) below T_{xy} .

spin-freezing transition. The physical reason for the marked change in magnetic properties of these alloys with relatively small changes in composition seems to be that the distribution of exchange integrals is very sensitive to nearest-neighbor distance, changing sign from positive to negative below about 0.25 nm. An increasing proportion of antiferromagnetic bonds with x destroys ferromagnetism and stabilizes an asperomagnetic ground state. Fully hydrogenated samples are all good ferromagnets.

ACKNOWLEDGMENTS

The 19-T magnetization curves were obtained at the Service National des Champs Intenses, Grenoble. We are grateful to Mr. E. Devlin for assistance with the ac susceptibility measurements and to Dr. J. M. Cadogan for help with the computer analysis. This work was supported in part by the European Commission under Contract No. SUM.041.EIR and grants from Trinity Trust, the Natural Science and Engineering Council of Canada, and Les Fonds pour la Formation des Chercheurs et à l'aide à Recherche of the Province of Quebec.

¹J. M. D. Coey and D. H. Ryan, IEEE Trans. Magn. **MAG-20**, 1278 (1984).

²T. Kemeny, F. J. Litterst, I. Vincze, and R. Wäppling, J. Phys. F **13**, L37 (1983).

³C. L. Chien and K. M. Unruh, Nucl. Instrum. Methods **199**, 193 (1982).

⁴K. M. Unruh and C. L. Chien, J. Magn. Magn. Mater. **31-34**, 1587 (1983).

⁵S. H. Liou, G. Xiao, J. N. Taylor, and C. L. Chien, J. Appl. Phys. **57**, 3536 (1985).

⁶J. M. D. Coey, D. Givord, A. Liénard, and J. P. Rebouillat, J. Phys. F **11**, 2707 (1981).

⁷K. Moorjani and J. M. D. Coey, *Metallic Glasses* (Elsevier, Amsterdam, 1984).

sterdam, 1984).

⁸H. Hiroyoshi and K. Fukamichi, Phys. Lett. **85A**, 242 (1981).

⁹S. N. Kaul, Phys. Rev. B **27**, 6923 (1983).

¹⁰D. A. Read, T. Moyo, and G. C. Hallam, J. Magn. Magn. Mater. **44**, 279 (1984).

¹¹J. A. Heller, E. F. Wassermann, M. F. Braun, and R. A. Brand, J. Magn. Magn. Mater. **54-57**, 307 (1986).

¹²W. Beck and H. Kronmüller, Phys. Status Solidi B **132**, 449 (1985).

¹³D. A. Read, T. Moyo, and G. C. Hallam, J. Magn. Magn. Mater. **54-57**, 309 (1986).

¹⁴R. Krishnan, K. V. Rao, and H. H. Liebermann, J. Appl. Phys. **55**, 1823 (1984).

- ¹⁵T. Masumoto, S. Ohnuma, K. Shirakawa, M. Nose, and K. Kobayashi, *J. Phys. (Paris) Colloq.* **41**, C8-686 (1980).
- ¹⁶Yu Boliang, D. H. Ryan, J. M. D. Coey, Z. Altounian, J. O. Ström-Olsen, and F. Razavi, *J. Phys. F* **13**, L217 (1983). We were unable to reproduce this result on other samples of the same composition.
- ¹⁷M. Ghafari, U. Gonser, H. G. Wagner, and M. Naka, *Nucl. Instrum. Methods* **199**, 197 (1982).
- ¹⁸A. H. Morrish, R. J. Pollard, Z. S. Wronski, and A. Cullen, *Phys. Rev. B* **32**, 7528 (1985).
- ¹⁹J. J. Rhyne and G. E. Fish, *J. Appl. Phys.* **57**, 3407 (1985).
- ²⁰H. Yamauchi, H. Onodera, and H. Yamamoto, *J. Phys. Soc. Jpn.* **53**, 747 (1984).
- ²¹S. N. Kaul, A. Hofmann, and H. Krönmüller, *J. Phys. F* **16**, 365 (1986).
- ²²J. M. D. Coey, D. H. Ryan, D. Gignoux, A. Liénard, and J. P. Rebouillat, *J. Appl. Phys.* **53**, 7804 (1982).
- ²³H. Fujimori, K. Nakanishi, H. Hiroyoshi, and N. S. Kazama, *J. Appl. Phys.* **53**, 7792 (1982).
- ²⁴J. M. D. Coey, D. H. Ryan, and Yu Boliang, *J. Appl. Phys.* **55**, 1800 (1984).
- ²⁵Z. S. Wronski, X. Z. Zhou, A. H. Morrish, and A. M. Stewart, *J. Appl. Phys.* **57**, 3548 (1985).
- ²⁶J. M. D. Coey, D. H. Ryan, Z. Altounian, P. Morin, and J. O. Ström-Olsen, in *Rapidly Quenched Metals*, edited by S. Steeb and H. Warlimont (Elsevier, Amsterdam, 1985), p. 1573.
- ²⁷Z. Altounian, E. Batalla, and J. O. Ström-Olsen, *J. Appl. Phys.* **59**, 2364 (1986).
- ²⁸D. H. Ryan and J. M. D. Coey, *J. Phys. E* **19**, 693 (1986).
- ²⁹B. Window, *J. Phys. F* **4**, 401 (1971).
- ³⁰H. Yamamoto, H. Onodera, K. Hosoyama, T. Masumoto, and H. Yamauchi *J. Magn. Magn. Mater.* **31-34**, 1579 (1983).
- ³¹H. Maeda, H. Terauchi, N. Kamijo, M. Hida, and K. Osamura, in *Proceedings of the 4th International Conference on Rapidly Quenched Metals, Sendai, 1981*, edited by T. Masumoto and K. Suzuki (Institute of Metals, Sendai, 1981), p. 397.
- ³²M. Gabay and G. Toulouse, *Phys. Rev. Lett.* **47**, 201 (1981).
- ³³N. Saito, H. Hiroyoshi, K. Fukamichi, and Y. Nakagawa, *J. Phys. F* **16**, 911 (1986).
- ³⁴I. A. Campbell, S. Senoussi, F. Varret, J. Teillet, and A. Hamzic, *Phys. Rev. Lett.* **50**, 1615 (1983).
- ³⁵R. A. Brand, V. Manns, and W. Keune, in *Heidelberg Colloquium on Spin Glasses*, Vol 192 of *Lecture Notes in Physics* (Springer-Verlag, Berlin, 1983), p. 79.
- ³⁶U. Mizutani, M. Matsuura, and K. Fukamichi, *J. Phys. F* **14**, 731 (1984).
- ³⁷J. M. D. Coey, D. H. Ryan, and R. Buder, *Phys. Rev. Lett.* **58**, 385 (1987).
- ³⁸D. Sherrington and S. Kirkpatrick, *Phys. Rev. Lett.* **35**, 1792 (1975).
- ³⁹S. Crane, D. W. Carnegie, Jr., and H. Claus, *J. Appl. Phys.* **53**, 2179 (1979).
- ⁴⁰I. A. Campbell, *Hyperfine Interact.* **27**, 15 (1986).
- ⁴¹C. N. Guy and J. O. Ström-Olsen, *J. Appl. Phys.* **50**, 1667 (1979).
- ⁴²H. Hiroyoshi and K. Fukamichi, *J. Appl. Phys.* **53**, 2226 (1982).